

Performance of QAM Schemes with Dual-Hop DF Relaying Systems over Mixed η - μ and κ - μ Fading Channels

Dharmendra Dixit and P. R. Sahu *Member, IEEE*

Abstract

Performance of quadrature amplitude modulation (QAM) schemes is analyzed with dual-hop decode-and-forward (DF) relaying systems over mixed η - μ and κ - μ fading channels. Closed-form expressions are obtained for the average symbol error rate (ASER) for general order rectangular QAM and cross QAM schemes using moment generating function based approach. Derived expressions are in the form of Lauricella's $(F_D^{(n)}(\cdot), \Phi_1^{(n)}(\cdot))$ hypergeometric functions which can be numerically evaluated using either integral or series representation. The obtained ASER expressions include other mixed fading channel cases addressed in the literature as special cases such as mixed Hoyt, and Rice fading, mixed Nakagami- m , and Rice fading. We further obtain a simple expression for the asymptotic ASER, which is useful to determine a factor governing the system performance at high SNRs, i.e., the diversity order. Additionally, we analyze the optimal power allocation, which provides a practical design rule to optimally distribute the total transmission power between the source and the relay to minimize the ASER. Extensive numerical and computer simulation results are presented that confirm the accuracy of presented mathematical analysis.

Index Terms

Quadrature amplitude modulation, average symbol error rate, decode-and-forward, dual-hop relaying, mixed fading, optimal power allocation.

Authors are with the School of Electrical Sciences, Indian Institute of Technology Bhubaneswar, Orissa, India (e-mail: dd12, prs)@iitbbs.ac.in.

I. INTRODUCTION

Cooperative communication has received considerable attention for several emerging wireless network architectures, such as cellular networks, local area networks and heterogeneous networks to counter the effect of multipath fading which degrades the symbol error rate (SER) performance [1]- [5]. The cooperative communication offers significant increase in capacity and multiplexing gain in the aforementioned wireless networks where user systems and nodes in a wireless network share their resources and create collaboration through distributed transmission. The motivation behind the cooperative communication is to provide virtual multiple-input multiple-output (MIMO) support for a user system which cannot accommodate multiple antenna due to size, complexity, power consumption and many other constraints. In a cooperative communication system, user terminals work as information sources as well as relays. The two main relaying methods used in cooperative communication scheme are amplify-and-forward (AF) and decode-and-forward (DF). In the AF case, the relay amplifies a signal transmitted by the source and then re-transmits the same to the destination. In the DF case, the relay decodes a signal transmitted by the source and then encodes and transmits to the destination.

In recent years, there has been an increased interest on the performance analysis of dual-hop cooperative communication networks where links are subject to asymmetric fading conditions [6]- [17] in which the propagation in one of the links is dominated by a strong line-of-sight (LOS) component relative to other links in the channel [18]. The performance analysis of dual-hop AF relay networks over mixed fading conditions are available in [6]- [13] and the analysis for dual-hop DF relay networks over mixed fading conditions are studied in [15]- [17]. In [17], authors present exact SER expressions of M -ary phase shift keying (MPSK) scheme for DF relay system over κ - μ and η - μ and mixed κ - μ and η - μ fading channels. However, no closed-form SER expression of MPSK in mixed κ - μ and η - μ fading channels has been provided. There are a number of works reported on the performance of the DF cooperative diversity over fading channels focusing on the capacity, diversity gain, and outage behavior of the system. Past few years has seen a research interest on the investigation of error performance of various modulation schemes for the DF cooperative diversity over general fading channels. In [19] and [20], SER performance for DF cooperation is examined over Rayleigh fading channels. The SER performance of different modulation schemes for dual-hop DF cooperation systems have

been derived over Nakagami- m fading channels in [21]- [24]. In [21], the end-to-end bit error rate (BER) performance of cooperative diversity networks using DF relaying over independent non-identical flat Nakagami- m fading channels is available. The SER expressions of MPSK and quadrature amplitude modulation (QAM) schemes for DF cooperative communications over Nakagami- m are derived in [22]. In [23], average BER performance of DF cooperative systems is investigated for binary PSK (BPSK) signals in Nakagami- m fading channels for integer values of m . Error probability of opportunistic DF relaying in Nakagami- m fading channels with arbitrary m is given in [24]. The authors in [25] present the outage and error rate performance analysis of the DF cooperative diversity system with OSTBC over spatially correlated Nakagami- m fading channels for integer values of m . The error performance of MPSK and square QAM (SQAM) signals for dual-hop DF cooperation systems have been investigated over two-wave with diffuse power fading channels in [26]. In [27], authors analyze the performance of SQAM schemes with DF relaying system over Hoyt (Nakagami- q) fading channels. In [28], the exact SER of M -ary PSK for multihop communication systems with regenerative relays is provided. In [29], the outage probability (OP), SER, level crossing rate and average outage duration are derived for multihop DF cooperation systems over Generalized- K fading channels. The OP and BER of Gray-coded rectangular QAM (RQAM) signals for multihop DF cooperative systems have been analyzed over η - μ fading channels in [30]. A closed-form expression for the OP of dual-hop DF relaying in dissimilar Rayleigh fading channels is derived in [31]. The authors in [32] and [33] are investigated the OP for the dual-hop DF protocol over Nakagami- m fading channels. The OP and outage capacity of dual-hop DF relaying system over η - μ and κ - μ channels are given in [34] and [35], respectively.

It is well known that the classical small-scale fading models (e.g., Rice, Hoyt, Nakagami- m) are not able to accurately characterize the small-scale variation of the fading signals, particularly at the tail probability [36]. Yacoub addressed this problem suggesting two new distributions for fading models namely η - μ and κ - μ which better accommodates practical situations for which classical distributions are a poor fit. The η - μ distribution accurately models small-scale fading for various non-LOS (NLOS) conditions including the Hoyt, and Nakagami- m distributions as special cases. On the other hand, the κ - μ distribution is a generalized distribution for modeling a great variety of LOS channels and includes Rice and Nakagami- m distributions as special cases. Some available works on performance analysis issues of cooperative systems operating in

these two generic fading channel models are available in [13], [17], [30], [34], [35] where the performance of AF and DF cooperative systems are investigated.

QAM is a promising modulation scheme for a digital multimedia transmission in wireless communications due to its high bandwidth efficiency [37]. RQAM, SQAM and cross QAM (XQAM) are well known QAM schemes among which RQAM is a generic modulation scheme which includes SQAM, binary PSK (BPSK), orthogonal binary frequency-shift keying, quadrature PSK (QPSK) and multilevel amplitude shift-keying modulation schemes as special cases. XQAM is an optimal QAM constellation for odd number of bits per symbol as it has low average symbol energy than RQAM [38]. XQAM finds application with constellations from 5 bits to 15 bits with usage in asymmetric digital subscriber lines and very high speed digital subscriber lines. Specifically, 32 and 128-XQAMs are employed in digital video broadcasting-cable. Moreover, XQAMs have been found to be useful in blind equalization [39] and adaptive modulation [40], [41].

Despite many research works dealing with the DF cooperative diversity during the past few years, to the best of our knowledge, closed-form expressions for the average SER (ASER) of general order RQAM and XQAM schemes with dual-hop DF relaying systems over mixed η - μ and κ - μ fading channels is not available in literature. In this paper, we derive novel closed-form expressions for the ASER for general order RQAM and XQAM schemes with dual-hop DF relaying systems operating over mixed η - μ and κ - μ fading channels. The obtained ASER expressions contain special functions such as Lauricella's ($F_D^{(n)}(\cdot)$, $\Phi_1^{(n)}(\cdot)$) hypergeometric functions which can be easily evaluated numerically using their finite integral or converging infinite series representation [42]- [46]. It is worth mentioning here that the derived expressions include the ASER expressions for mixed Hoyt, and Rice fading, mixed Nakagami- m and Rice fading, and non-identical Nakagami- m fading as special cases. We further derive a simple expression for the asymptotic ASER, which is useful to determine a factor governing the system performance at high SNRs, i.e., the diversity order. Additionally, we obtain the optimal power allocation factor, which provides a practical design rule to optimally distribute the total transmission power between the source and the relay to minimize the ASER.

The rest of the paper is organized as follows. Section II deals with system and channel models and the ASER expressions are derived in Section III. In Section IV, numerical results and discussion are given. The paper is concluded in Section V.

II. SYSTEM AND CHANNEL MODELS

We consider a three-node system model [22]. This model finds a typical application of cooperative communications for the uplink of cellular wireless systems. This type of cooperative communication is also suitable for handsets equipped with single antenna for achieving transmit spatial diversity for link-quality improvement. In this system model, the source node s sends its information to the destination node d on two consecutive time slots. In the first time slot, node s broadcasts its symbol to node d and relay node r . In the second time slot, only node r , if decodes successfully, forwards the received symbol to node d . In this paper, we assume that the relay can successfully decode if the SNR level of the sr link is above a predetermined threshold. In a single relay dual-hop DF relaying system, node i sends its information to node j over ij link, where $i \in \{s, r\}$, $j \in \{r, d\}$ and $ij \in \{sd, sr, rd\}$. When unit energy symbol x is transmitted from node i , the baseband signal received at node j can be given as

$$y_{ij} = \sqrt{\tilde{P}_i} \alpha_{ij} x + n_{ij} \quad (1)$$

where \tilde{P}_i is the power of the transmitted signal at node i , α_{ij} denotes fading channel coefficient of ij link which is modeled as either η - μ or κ - μ distribution, n_{ij} is additive white Gaussian noise (AWGN) with N_0 variance at node j . At node s the symbol is transmitted with power $\tilde{P}_i = P_s$. If node r successfully decodes the received symbol, the symbol is transmitted with power $\tilde{P}_i = P_r$, otherwise node r remains idle, i.e. $P_r = 0$. The total power P of this dual-hop DF relaying system is given by $P = P_s + P_r$, $0 < P_s, P_r < P$. Finally, node d combines the signals of both the time slots according to maximal ratio combining (MRC) technique.

The instantaneous SNR, γ_{ij} of ij link is defined as $\gamma_{ij} = \alpha_{ij}^2 \tilde{P}_i / N_0$. If a link is subjected to η - μ fading, the probability density function (PDF) of γ_{ij} can be expressed as [36]

$$f_{\gamma_{ij}}(\gamma) = \frac{2\sqrt{\pi} \mu_{ij}^{\mu_{ij} + \frac{1}{2}} h_{ij}^{\mu_{ij}} \gamma^{\mu_{ij} - \frac{1}{2}}}{\Gamma(\mu_{ij}) H_{ij}^{\mu_{ij} - \frac{1}{2}} \bar{\gamma}_{ij}^{\mu_{ij} + \frac{1}{2}}} \exp\left(-\frac{2\mu_{ij} h_{ij} \gamma}{\bar{\gamma}_{ij}}\right) I_{\mu_{ij} - \frac{1}{2}}\left(\frac{2\mu_{ij} H_{ij} \gamma}{\bar{\gamma}_{ij}}\right), \quad (2)$$

where $\Gamma(\cdot)$ is the gamma function, $I_\nu(\cdot)$ is the modified Bessel function of the first kind and ν th order, μ_{ij} denotes the number of multipath clusters, and both h_{ij} and H_{ij} are functions of η_{ij} . In (2), $\bar{\gamma}_{ij} = \mathbb{E}[\gamma_{ij}] = \Omega_{ij} \tilde{P}_i / N_0$ denotes the average SNR of the ij link, where $\mathbb{E}[\cdot]$ is

the expectation operator and $\Omega_{ij} = \mathbb{E}[\alpha_{ij}^2]$ is the variance of α_{ij} . The distribution in (2) has been described for two types of physical models (Formats) depending on the way the parameter η_{ij} is defined. In this paper, we consider only Format 1. In Format 1, $0 < \eta_{ij} < \infty$ is the ratio of the power of inphase and quadrature phase components of the scatter wave signals in each multipath cluster, with $h_{ij} = (2 + \eta_{ij}^{-1} + \eta_{ij})/4$ and $H_{ij} = (\eta_{ij}^{-1} - \eta_{ij})/4$. It includes Hoyt ($\eta_{ij} = q^2$, $\mu_{ij} = 0.5$), and Nakagami- m ($\eta_{ij} = 1$, $\mu_{ij} = m/2$) as special cases. The analysis presented here can also be extended to Format 2.

If a link is subjected to κ - μ fading, the PDF of γ_{ij} can be expressed as [36]

$$f_{\gamma_{ij}}(\gamma) = \frac{\mu_{ij}(1 + \kappa_{ij})^{\frac{\mu_{ij}+1}{2}} \gamma^{\frac{\mu_{ij}-1}{2}}}{\bar{\gamma}_{ij}^{\frac{\mu_{ij}+1}{2}} \kappa_{ij}^{\frac{\mu_{ij}-1}{2}} \exp(\mu_{ij}\kappa_{ij})} \exp\left(-\frac{(1 + \kappa_{ij})\gamma}{\mu_{ij}^{-1}\bar{\gamma}_{ij}}\right) \quad (3)$$

where $\kappa_{ij} > 0$ denotes the ratio of the total power due to dominant components to the total power due to scattered waves. This fading includes Rice ($\mu_{ij} = 1$ and $\kappa_{ij} = K$), and Nakagami- m ($\kappa_{ij} \rightarrow 0$ and $\mu_{ij} = m$) as special cases.

Let γ_{th} be the predetermined threshold for the sr link. If instantaneous SNR γ_{sr} of sr link falls below γ_{th} , the link from node s to node d via node r is assumed to fail. On the other hand, if node r can successfully decode the messages from node s and forwards to node d , then the PDF of the end to end SNR γ_{srd} can be given as [29], [31]

$$f_{\gamma_{srd}}(\gamma) = A_{sr}\delta(\gamma) + (1 - A_{sr})f_{\gamma_{rd}}(\gamma), \quad (4)$$

where A_{sr} is the probability that outage occurs in sr link and $\delta(\cdot)$ is Dirac delta function. The probability A_{sr} in (4) can be calculated as [29]

$$A_{sr} = 1 - \Pr\{\gamma_{sr} > \gamma_{th}\} = F_{\gamma_{sr}}(\gamma_{th}), \quad (5)$$

where $\Pr\{\cdot\}$ is the probability operation and $F_{\gamma_{sr}}(\cdot)$ denotes the cumulative distribution of function of γ_{sr} .

III. AVERAGE SYMBOL ERROR RATE ANALYSIS

Mathematically, ASER $P(e)$ of any modulation scheme for considered system can be computed as [49]

$$P(e) = \int_0^\infty P(e|\gamma)f_{\gamma_t}(\gamma)d\gamma, \quad (6)$$

where $P(e|\gamma)$ is the conditional SER of the modulation scheme in AWGN channels and $f_{\gamma_t}(\gamma)$ is the PDF of the total SNR γ_t of output of the MRC combiner at node d . To obtain the closed-form ASER expression, the moment generating function (MGF) of γ_t is required. The γ_t can be given as [49]

$$\gamma_t = \gamma_{sd} + \gamma_{srd}. \quad (7)$$

The MGF of γ_u is defined as [49]

$$\mathcal{M}_{\gamma_u}(z) = \int_0^\infty \exp(-z\gamma) f_{\gamma_u}(\gamma) d\gamma, \quad (8)$$

where $u \in \{sd, rd, srd, t\}$, and z is the Laplace variable. The $\mathcal{M}_{\gamma_t}(z)$ of γ_t can be obtained from the formula [49]

$$\mathcal{M}_{\gamma_t}(z) = \mathcal{M}_{\gamma_{sd}}(z) \mathcal{M}_{\gamma_{srd}}(z). \quad (9)$$

Using (4) in (8), the expression of $\mathcal{M}_{\gamma_{srd}}(z)$ can be obtained as [43]

$$\mathcal{M}_{\gamma_{srd}}(z) = A_{sr} + (1 - A_{sr}) \mathcal{M}_{\gamma_{rd}}(z), \quad (10)$$

Finally, substituting (10) in (9), $\mathcal{M}_{\gamma_t}(z)$ can be written as

$$\mathcal{M}_{\gamma_t}(z) = A_{sr} \mathcal{M}_{\gamma_{sd}}(z) + (1 - A_{sr}) \mathcal{M}_{\gamma_{sd}}(z) \mathcal{M}_{\gamma_{rd}}(z). \quad (11)$$

Using (2) in (8), the $\mathcal{M}_{\gamma_{ij}}(z)$ of η - μ faded ij link can be obtained as [43]

$$\mathcal{M}_{\gamma_{ij}}(z) = \frac{(4\mu_{ij}^2 h_{ij})^{\mu_{ij}} (2\mu_{ij}(h_{ij} + H_{ij}) + z\bar{\gamma}_{ij})^{-\mu_{ij}}}{(2\mu_{ij}(h_{ij} - H_{ij}) + z\bar{\gamma}_{ij})^{\mu_{ij}}}. \quad (12)$$

Using (3) in (8), the $\mathcal{M}_{\gamma_{ij}}(z)$ of κ - μ faded ij link can be obtained as [43]

$$\mathcal{M}_{\gamma_{ij}}(z) = \left(\frac{\mu_{ij}(1 + \kappa_{ij})}{\mu_{ij}(1 + \kappa_{ij}) + z\bar{\gamma}_{ij}} \right)^{\mu_{ij}} \exp \left(\frac{-z\mu_{ij}\kappa_{ij}\bar{\gamma}_{ij}}{\mu_{ij}(1 + \kappa_{ij}) + z\bar{\gamma}_{ij}} \right). \quad (13)$$

The scenario, where one hop of the link is subjected to η - μ fading and the other hop is subjected to κ - μ fading, can be modeled accurately by mixed NLOS and LOS conditions, which occur in various applications including micro-/macrocellular and/or hybrid satellite/terrestrial communication systems [14], [18]. We assume that all links experience independent and non

identical but asymmetric fading. With two different fading types, there are six possible combinations for mixed fading scenarios as given in Table I. We have analyzed the mixed fading scenario

TABLE I
FADING PARAMETERS OF DIFFERENT SCENARIOS.

Scenario	Links parameters		
	sd	sr	rd
1	η_{sd}, μ_{sd}	η_{sr}, μ_{sr}	κ_{rd}, μ_{rd}
2	κ_{sd}, μ_{sd}	η_{sr}, μ_{sr}	η_{rd}, μ_{rd}
3	κ_{sd}, μ_{sd}	κ_{sr}, μ_{sr}	η_{rd}, μ_{rd}
4	η_{sd}, μ_{sd}	κ_{sr}, μ_{sr}	κ_{rd}, μ_{rd}
5	κ_{sd}, μ_{sd}	η_{sr}, μ_{sr}	κ_{rd}, μ_{rd}
6	η_{sd}, μ_{sd}	κ_{sr}, μ_{sr}	η_{rd}, μ_{rd}

1 where γ_{sd} and γ_{sr} are modeled as η - μ distribution but γ_{rd} is modeled as κ - μ distribution. For η - μ faded sr link A_{sr} can be given as [47]

$$A_{sr} = 1 - Y_{\mu_{sr}} \left(\frac{H_{sr}}{h_{sr}}, \sqrt{\frac{2\mu_{sr}h_{sr}\gamma_{th}}{\gamma_{sr}}} \right), \quad (14)$$

where $Y_{\nu}(a, b) = \frac{2^{\frac{3}{2}-\nu} \sqrt{\pi}(1-a^2)^{\nu}}{a^{\nu-\frac{1}{2}}\Gamma(\nu)} \int_b^{\infty} x^{2\nu} e^{-x^2} I_{\nu-\frac{1}{2}}(ax^2) dx$ is the Yacoub's integral [36]. A general solution of this integral is [47]

$$Y_{\nu}(a, b) = 1 - \frac{\Phi_2^{(2)}(\nu, \nu; 1 + 2\nu; -(1+a)b^2, -(1-a)b^2)}{(1-a^2)^{-\nu} b^{-4\nu} \Gamma(1+2\nu)}, \quad (15)$$

where $\Phi_2^{(2)}$ is the confluent Lauricella function [48]. In [47], another closed-form expression for the integer values of $2\mu_{sr}$ is also presented.

A. Exact Analysis

1) *M*-ary RQAM : The conditional SER performance of $M = M_I \times M_Q$ -ary RQAM in AWGN channels is given as [44], [50]

$$\begin{aligned} P(e|\gamma) &= 2p Q(a\sqrt{\gamma}, \pi/2) + 2q Q(b\sqrt{\gamma}, \pi/2) - 2pq \{ Q(a\sqrt{\gamma}, \operatorname{arccot}(b/a)) \\ &\quad + Q(b\sqrt{\gamma}, \operatorname{arctan}(b/a)) \}, \end{aligned} \quad (16)$$

where $p = 1 - \frac{1}{M_I}$, $q = 1 - \frac{1}{M_Q}$, M_I and M_Q are the number of in-phase and quadrature-phase constellation points, respectively, $a = \sqrt{\frac{6}{(M_I^2-1)+(M_Q^2-1)\beta^2}}$, $b = \beta a$ and $\beta = d_Q/d_I$ is the quadrature-to-in-phase decision distance ratio with d_I and d_Q being the in-phase and quadrature decision distance, respectively, and $Q(x, \phi)$ is given as [42], [49]

$$Q(x, \phi) = \frac{1}{\pi} \int_0^\phi \exp\left(-\frac{x^2}{2 \sin^2 \theta}\right) d\theta; \quad x \geq 0. \quad (17)$$

Substituting (16) in (6) and by algebraic manipulations ASER for RQAM scheme denoted as $P^{\text{RQAM}}(e)$, can be expressed as

$$P^{\text{RQAM}}(e) = 2p \mathcal{I}(a, \pi/2) + 2q \mathcal{I}(b, \pi/2) - 2pq \{ \mathcal{I}(a, \text{arccot}(b/a)) + \mathcal{I}(b, \arctan(b/a)) \}, \quad (18)$$

where the function $\mathcal{I}(\cdot, \cdot)$ is defined as

$$\begin{aligned} \mathcal{I}(x, \phi) &= \int_0^\infty Q(x\sqrt{\gamma}, \phi) f_{\gamma_t}(\gamma) d\gamma \\ &= \frac{1}{\pi} \int_0^\phi \int_0^\infty \exp\left(-\frac{x^2 \gamma}{2 \sin^2 \theta}\right) f_{\gamma_t}(\gamma) d\gamma d\theta \\ &= \frac{1}{\pi} \int_0^\phi \mathcal{M}_{\gamma_t}\left(\frac{x^2}{2 \sin^2 \theta}\right) d\theta. \end{aligned} \quad (19)$$

Now, substituting (11) in (19), $\mathcal{I}(x, \phi)$ can be written as

$$\mathcal{I}(x, \phi) = A_{sr} \mathcal{I}_1(x, \phi) + (1 - A_{sr}) \mathcal{I}_2(x, \phi), \quad (20)$$

where

$$\mathcal{I}_1(x, \phi) = \frac{1}{\pi} \int_0^\phi \mathcal{M}_{\gamma_{sd}}\left(\frac{x^2}{2 \sin^2 \theta}\right) d\theta, \quad (21)$$

and

$$\mathcal{I}_2(x, \phi) = \frac{1}{\pi} \int_0^\phi \mathcal{M}_{\gamma_{sd}}\left(\frac{x^2}{2 \sin^2 \theta}\right) \mathcal{M}_{\gamma_{rd}}\left(\frac{x^2}{2 \sin^2 \theta}\right) d\theta. \quad (22)$$

The closed-form expressions for $\mathcal{I}_1(x, \phi)$ and $\mathcal{I}_2(x, \phi)$ are derived in Appendix. Thus, the ASER expression for $P^{\text{RQAM}}(e)$ can be given as

$$P^{\text{RQAM}}(e) = A_{sr} \{ 2p \mathcal{I}_1(a, \pi/2) + 2q \mathcal{I}_1(b, \pi/2) - 2p q \mathcal{I}_1(a, \text{arccot}(b/a)) - 2p q \mathcal{I}_1(b, \text{arctan}(b/a)) \} \\ + (1 - A_{sr}) \{ 2p \mathcal{I}_2(a, \pi/2) + 2q \mathcal{I}_2(b, \pi/2) - 2p q \mathcal{I}_2(a, \text{arccot}(b/a)) - 2p q \mathcal{I}_2(b, \text{arctan}(b/a)) \}. \quad (23)$$

For the special case of M -ary SQAM,¹ i.e. when $M_I = M_Q = \sqrt{M}$ and $\beta = 1$, it can be shown that (23) reduces to

$$P^{\text{SQAM}}(e) = 4A_{sr} \tilde{p} \{ \mathcal{I}_1(\tilde{a}, \pi/2) - \tilde{p} \mathcal{I}_1(\tilde{a}, \pi/4) \} + 4(1 - A_{sr}) \tilde{p} \{ \mathcal{I}_2(\tilde{a}, \pi/2) - \tilde{p} \mathcal{I}_2(\tilde{a}, \pi/4) \}, \quad (24)$$

where $\tilde{p} = 1 - \frac{1}{\sqrt{M}}$ and $\tilde{a} = \sqrt{\frac{3}{M-1}}$. For the special case of BPSK, i.e. when $M_I = 2$, $M_Q = 1$ and $\beta = 0$, it can be shown that (23) reduces to

$$P^{\text{BPSK}}(e) = A_{sr} \mathcal{I}_1(\sqrt{2}, \pi/2) + (1 - A_{sr}) \mathcal{I}_2(\sqrt{2}, \pi/2). \quad (25)$$

2) *M*-ary XQAM : The conditional SER performance of *M*-ary XQAM in AWGN channels can be given as [42]

$$P(e|\gamma) = g_1 Q(a_0 \sqrt{\gamma}, \pi/2) - g_2 \sum_{k=1}^{\nu-1} Q(a_k \sqrt{\gamma}, \arctan(k/(k+1))) \\ + g_2 Q(a_1 \sqrt{\gamma}, \pi/2) + g_2 \sum_{k=2}^{\nu} Q(a_k \sqrt{\gamma}, \arctan(k/(k-1))) \\ - g_3 Q(a_0 \sqrt{\gamma}, \pi/4) - 2g_2 \sum_{k=1}^{\nu-1} Q(a_0 \sqrt{\gamma}, \arctan(1/(2k+1))), \quad (26)$$

where $M = 32, 128, 512, \dots$, $g_1 = 4 - \frac{6}{\sqrt{2M}}$, $g_2 = \frac{4}{M}$, $g_3 = 4 - \frac{12}{\sqrt{2M}} + \frac{12}{M}$, $\nu = \frac{\sqrt{2M}}{8}$, $a_0 = \sqrt{\frac{96}{(31M-32)}}$, $a_k = \sqrt{2k}a_0$, $k = 1, 2, \dots, \nu$.

Using a similar approach as followed to obtained (23), a closed-form ASER expression of

¹Substitute $y = x$ into (42) and (44) to obtain $\mathcal{I}_1(x, \pi/4)$ and $\mathcal{I}_2(x, \pi/4)$, respectively

XQAM can be obtained as given

$$\begin{aligned}
P^{\text{XQAM}}(e) = & (1 - A_{sr}) \left\{ \mathcal{I}_2(a_0, \pi/2) + g_2 \mathcal{I}_2(a_1, \pi/2) \right\} + A_{sr} \left\{ \mathcal{I}_1(a_0, \pi/2) \right. \\
& - g_2 \sum_{k=1}^{\nu-1} \mathcal{I}_1(a_k, \arctan(k/(k+1))) + g_2 \mathcal{I}_1(a_1, \pi/2) + g_2 \sum_{k=2}^{\nu} \mathcal{I}_1(a_k, \arctan(k/(k-1))) \\
& - g_3 \mathcal{I}_1(a_0, \pi/4) - 2g_2 \sum_{k=1}^{\nu-1} \mathcal{I}_1(a_0, \arctan(1/(2k+1))) \left. \right\} + (1 - A_{sr}) \left\{ -g_3 \mathcal{I}_2(a_0, \pi/4) \right. \\
& g_2 \sum_{k=2}^{\nu} \mathcal{I}_2(a_k, \arctan(k/(k-1))) - 2g_2 \sum_{k=1}^{\nu-1} \mathcal{I}_2(a_0, \arctan(1/(2k+1))) \\
& \left. - g_2 \sum_{k=1}^{\nu-1} \mathcal{I}_2(a_k, \arctan(k/(k+1))) \right\}. \tag{27}
\end{aligned}$$

B. Asymptotic Analysis

In asymptotic analysis, we assume that the average SNR values for three links are sufficiently large i.e., $\bar{\gamma}_{ij} \gg 1$. With the high SNR assumption, the MGF of η - μ faded link in (12) can be approximated as

$$\mathcal{M}_{\gamma_{ij}}^{\infty}(z) \simeq \left(\frac{2\mu_{ij}\sqrt{h_{ij}}}{z\bar{\gamma}_{ij}} \right)^{2\mu_{ij}}, \tag{28}$$

and the MGF of κ - μ faded link in (13) can be approximated as

$$\mathcal{M}_{\gamma_{ij}}^{\infty}(z) \simeq \left(\frac{\mu_{ij}(1 + \kappa_{ij})}{z\bar{\gamma}_{ij}} \right)^{\mu_{ij}} \exp(-\mu_{ij}\kappa_{ij}). \tag{29}$$

Thus, A_{sr} of sr link can be approximated as

$$\begin{aligned}
A_{sr}^{\infty} & \simeq \mathcal{L}^{-1} \left\{ \frac{\mathcal{M}_{\gamma_{sr}}^{\infty}(z)}{z} \right\} \Big|_{\gamma=\gamma_{th}} \\
& \simeq \frac{1}{\Gamma(2\mu_{sr} + 1)} \left(\frac{2\mu_{sr}\sqrt{h_{sr}}\gamma_{th}}{\bar{\gamma}_{sr}} \right)^{2\mu_{sr}}, \tag{30}
\end{aligned}$$

where $\mathcal{L}^{-1}\{\cdot\}$ is the inverse Laplace transform operator. For high SNR, we can also assume $1 - A_{sr}^{\infty} \simeq 1$.

1) *M*-ary RQAM: Using (28), (29) and (30), the asymptotic ASER for RQAM, $P_{\infty}^{\text{RQAM}}(e)$ can be expressed as

$$\begin{aligned} P_{\infty}^{\text{RQAM}}(e) = & A_{sr}^{\infty} \left\{ 2p \mathcal{I}_1^{\infty}(a, \pi/2) + 2q \mathcal{I}_1^{\infty}(b, \pi/2) - 2p q \mathcal{I}_1^{\infty}(a, \text{arccot}(b/a)) \right. \\ & - 2p q \mathcal{I}_1^{\infty}(b, \arctan(b/a)) \left. \right\} - 2p q \mathcal{I}_2^{\infty}(a, \text{arccot}(b/a)) - 2p q \mathcal{I}_2^{\infty}(b, \arctan(b/a)) \\ & + 2p \mathcal{I}_2^{\infty}(a, \pi/2) + 2q \mathcal{I}_2^{\infty}(b, \pi/2), \end{aligned} \quad (31)$$

where

$$\mathcal{I}_1^{\infty}(x, \phi) = \frac{1}{\pi} \int_0^{\phi} \mathcal{M}_{\gamma_{sd}}^{\infty} \left(\frac{x^2}{2 \sin^2 \theta} \right) d\theta, \quad (32)$$

and

$$\mathcal{I}_2^{\infty}(x, \phi) = \frac{1}{\pi} \int_0^{\phi} \mathcal{M}_{\gamma_{sd}}^{\infty} \left(\frac{x^2}{2 \sin^2 \theta} \right) \mathcal{M}_{\gamma_{rd}}^{\infty} \left(\frac{x^2}{2 \sin^2 \theta} \right) d\theta. \quad (33)$$

The closed-form expressions for $\mathcal{I}_1^{\infty}(x, \phi)$ and $\mathcal{I}_2^{\infty}(x, \phi)$ are derived in Appendix.

2) *M*-ary XQAM: Using an approach similar to that followed to obtain (31), a closed-form asymptotic ASER expression for XQAM can be given as

$$\begin{aligned} P_{\infty}^{\text{XQAM}}(e) = & A_{sr}^{\infty} \left\{ \mathcal{I}_1^{\infty}(a_0, \pi/2) - g_2 \sum_{k=1}^{\nu-1} \mathcal{I}_1^{\infty}(a_k, \arctan(k/(k+1))) \right. \\ & + g_2 \mathcal{I}_1^{\infty}(a_1, \pi/2) + g_2 \sum_{k=2}^{\nu} \mathcal{I}_1^{\infty}(a_k, \arctan(k/(k-1))) \\ & - g_3 \mathcal{I}_1^{\infty}(a_0, \pi/4) - 2g_2 \sum_{k=1}^{\nu-1} \mathcal{I}_1^{\infty}(a_0, \arctan(1/(2k+1))) \left. \right\} \\ & + \left\{ \mathcal{I}_2^{\infty}(a_0, \pi/2) - g_2 \sum_{k=1}^{\nu-1} \mathcal{I}_2^{\infty}(a_k, \arctan(k/(k+1))) \right. \\ & + g_2 \mathcal{I}_2^{\infty}(a_1, \pi/2) + g_2 \sum_{k=2}^{\nu} \mathcal{I}_2^{\infty}(a_k, \arctan(k/(k-1))) \\ & - g_3 \mathcal{I}_2^{\infty}(a_0, \pi/4) - 2g_2 \sum_{k=1}^{\nu-1} \mathcal{I}_2^{\infty}(a_0, \arctan(1/(2k+1))) \left. \right\}. \end{aligned} \quad (34)$$

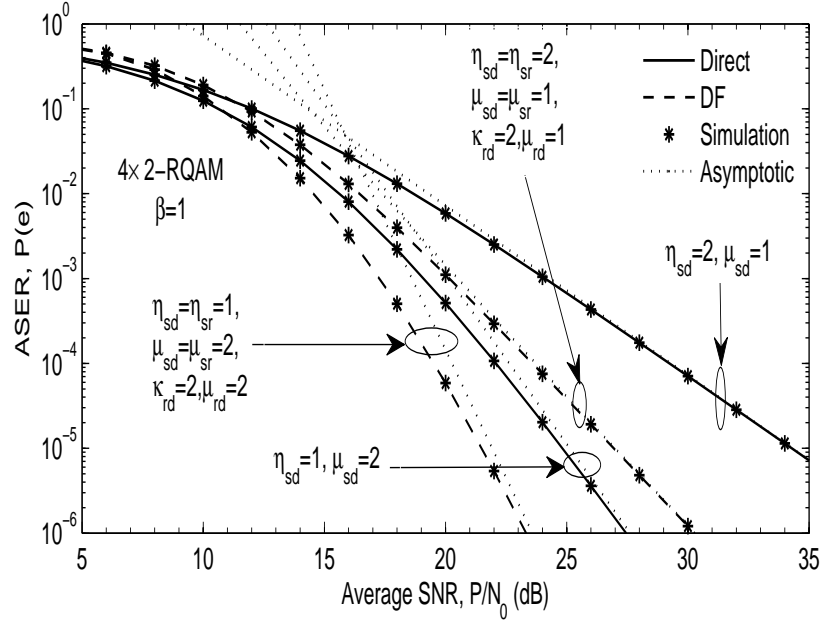


Fig. 1. ASER of 4×2 -RQAM scheme with varying η , κ and μ .

The asymptotic ASER expressions in (31) and (34) can be rewritten by substituting $P_s = \xi P$ and $P_r = (1 - \xi)P$ for $0 \leq \xi \leq 1$, as

$$P_{\infty}^{\text{QAM}}(e) = \mathcal{E}_1 \left(\frac{P}{N_0} \right)^{-2(\mu_{sd} + \mu_{sr})} + \mathcal{E}_2 \left(\frac{P}{N_0} \right)^{-(2\mu_{sd} + \mu_{rd})} \quad (35)$$

where \mathcal{E}_1 and \mathcal{E}_2 summarize the necessary elements in the asymptotic ASER expressions. The ξ is optimal power allocation factor.

C. Diversity Order Analysis

The diversity order, \mathcal{O}_{DF} of dual-hop DF relaying system can be calculated as [51]

$$\mathcal{O}_{\text{DF}} = \lim_{\frac{P}{N_0} \rightarrow \infty} \frac{-\log P^{\text{QAM}}(e)}{\log \frac{P}{N_0}} \quad (36)$$

Using (35) and (36), we can show that our considered scenario 1 (in Table I) of this system achieves the maximum diversity order of $\mathcal{O}_{\text{DF}} = 2\mu_{sd} + \min\{2\mu_{sr}, \mu_{rd}\}$. It can be observed that the fading parameters η_{sd} , η_{sr} and κ_{rd} have no impact on the diversity order.

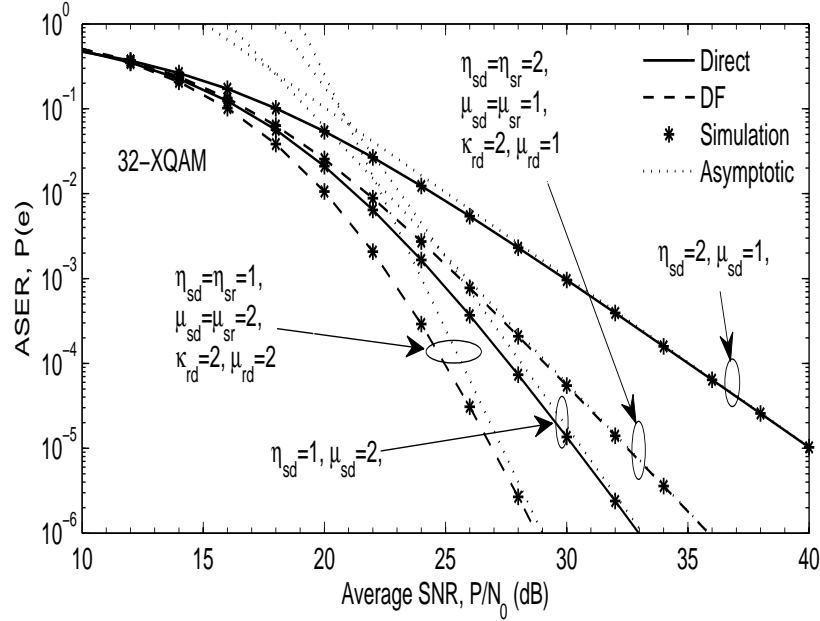


Fig. 2. ASER of 32-QAM scheme with varying η , κ and μ .

D. Optimal Power Allocation Analysis

Equal power allocation strategy for transmitters is not an optimal solution for power allocation. If partial channel state information is available at the transmitting nodes, an optimal power allocation can be performed to minimize the ASER at the destination node [22]. The asymptotic ASER expressions in (31) and (34) can be rewritten by substituting $P_s = \xi P$ and $P_r = (1 - \xi)P$ for $0 \leq \xi \leq 1$, as

$$P_{\infty}^{\text{QAM}}(\xi) = \frac{\Omega_{sd}^{-2\mu_{sd}} \Omega_{sr}^{-2\mu_{sr}} \mathcal{C}_1}{\xi^{2(\mu_{sd} + \mu_{sr})}} + \frac{\Omega_{sd}^{-2\mu_{sd}} \xi^{-2\mu_{sd}} \mathcal{C}_2}{\Omega_{rd}^{\mu_{rd}} (1 - \xi)^{\mu_{rd}}}, \quad (37)$$

where $\mathcal{C}_1, \mathcal{C}_2 \geq 0$ are constants of the expression². It can be shown that the second derivative of (37) w.r.t ξ is always greater than or equal to 0, i.e., $d^2 P_{\infty}^{\text{QAM}}(\xi) / d\xi^2 \geq 0$. Hence (37) is a convex function w.r.t. ξ . Equating the first derivative of (37) w.r.t. ξ to zero, we get the relation

$$-2\mathcal{C}_1(\mu_{sd} + \mu_{sr})\Omega_{rd}^{\mu_{rd}}(1 - \xi)^{\mu_{rd}+1} = \mathcal{C}_2\Omega_{sr}^{2\mu_{sr}}\xi^{2\mu_{sr}}(2\mu_{sd} - (2\mu_{sd} + \mu_{rd})\xi). \quad (38)$$

²not given here as it is not required for optimization

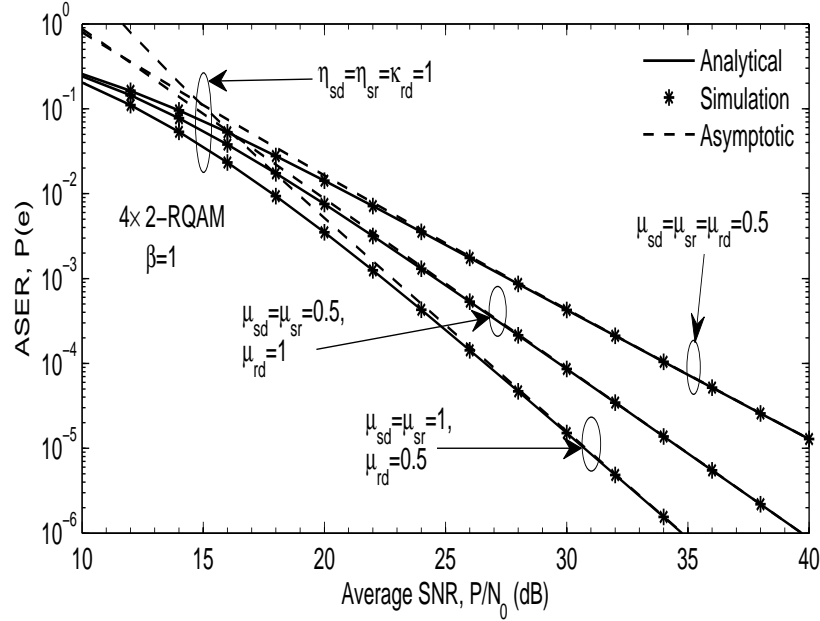


Fig. 3. ASER of 4×2 -RQAM scheme for dual-hop DF relaying system with varying μ and fixed $\eta = \kappa = 1$.

It can be observed from (38) that the asymptotic optimum power allocation does not depend on the variance of link between s and d , it depends only on the variances of links between s and r and, between r and d . Moreover, we can also infer that the optimum transmitted power P_s at s is larger than $2\mu_{sd}P/(2\mu_{sd} + \mu_{rd})$ and less than P , while the optimum power P_r used at r is larger than 0 and less than $\mu_{rd}P/(2\mu_{sd} + \mu_{rd})$. It means that we should always allocate more power at s and less power at r .

IV. NUMERICAL RESULTS AND DISCUSSION

Numerical examples concerning the ASER performance of QAM schemes are presented with computer simulations to verify the accuracy of analytical results. The Lauricella's hypergeometric functions are numerically evaluated using their finite integral representation. In the numerical evaluation, we assume that the power is equally allocated to the source and the relay and the variance of each link is unity, i.e., $\Omega_{sd} = \Omega_{sr} = \Omega_{rd} = 1$, unless stated otherwise. Additionally, the threshold γ_{th} is chosen according to $\gamma_{th} = 2^{2R} - 1$, with the spectrum efficiency R being set to 1 bit/s/Hz.

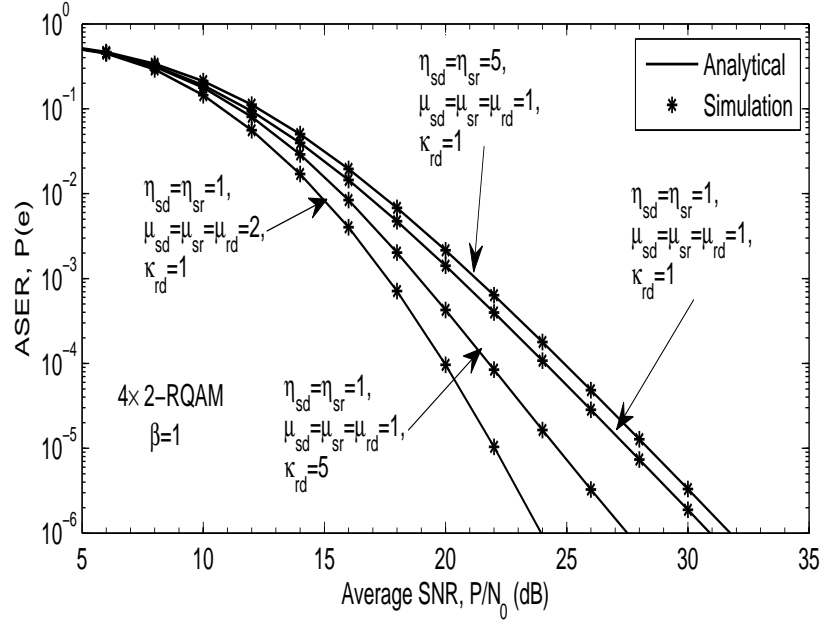


Fig. 4. ASER of 4×2 -RQAM scheme for dual-hop DF relaying system with varying η , κ and μ .

A. Direct Communication versus DF Cooperative Communication with RQAM and XQAM Schemes

Figs. 1, and 2 illustrate the ASER for 4×2 -RQAM, and 32 -XQAM schemes, respectively. We notice that the numerical results match with the corresponding computer simulation results. These figures also show that the DF cooperative communication can always substantially improve the ASER performance, relative to the direct communication over the medium-to-high SNR region. For example, it can be observed from Fig. 1 that for an ASER of 10^{-4} , P/N_0 improvement that can be achieved in dual-hop DF relaying system ($\eta_{sd} = \eta_{sr} = 1$, $\mu_{sd} = \mu_{sr} = 2$, $\kappa_{rd} = 2$, $\mu_{rd} = 2$) over direct communication ($\eta_{sd} = 1$, $\mu_{sd} = 2$) is 3dB (approx.)

B. Impact of Fading Parameters

Fig. 3 shows the impact of $\mu_{sd} = \mu_{sr}$, and μ_{rd} for fixed $\eta_{sd} = \eta_{sr} = \kappa_{rd} = 1$ on the ASER of 4×2 -RQAM scheme for dual-hop DF relaying system over mixed η - μ and κ - μ fading channels. It can be observed from this figure that the SNR gains are achieved resulting from increasing the fading parameters, $\mu_{sd} = \mu_{sr}$, and μ_{rd} . For example, an ASER of 10^{-4} with $\eta_{sd} = \eta_{sr} = \kappa_{rd} = 1$ occurs at $P/N_0 \approx 34$ dB when $\mu_{sd} = \mu_{sr} = \mu_{rd} = 0.5$, $P/N_0 \approx 30$ dB when $\mu_{sd} = \mu_{sr} = 0.5$, and $\mu_{rd} = 1$, and, $P/N_0 \approx 26.5$ dB when $\mu_{sd} = \mu_{sr} = 1$, and $\mu_{rd} = 0.5$.

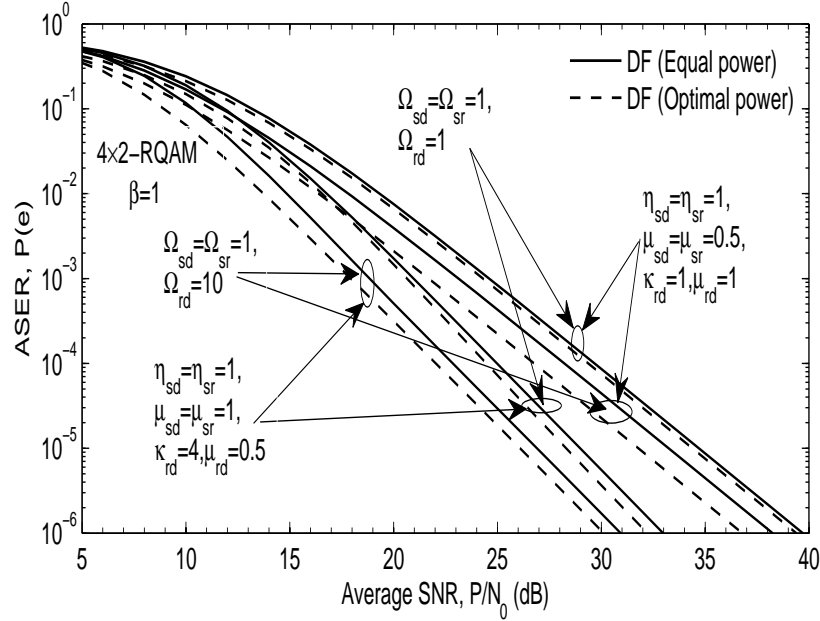


Fig. 5. ASER of 4×2 -RQAM scheme for dual-hop DF relaying system with equal and optimal allocation.

Fig. 4 shows the impact of η , κ and μ on the ASER of 4×2 -RQAM scheme for dual-hop DF relaying system. Two important observations can be drawn from this figure. First, the SNR gains are resulting from increasing the fading parameters, κ and μ , as expected. For example, an ASER of 10^{-4} occurs at $P/N_0 \approx 24$ dB when $\eta_{sd} = \eta_{sr} = 1$, $\mu_{sd} = \mu_{sr} = \mu_{rd} = 1$, and $\kappa_{rd} = 1$, $P/N_0 \approx 22$ dB when $\eta_{sd} = \eta_{sr} = 1$, $\mu_{sd} = \mu_{sr} = \mu_{rd} = 1$, and $\kappa_{rd} = 5$, and $P/N_0 \approx 20$ dB when $\eta_{sd} = \eta_{sr} = 1$, $\mu_{sd} = \mu_{sr} = \mu_{rd} = 2$, and $\kappa_{rd} = 1$. Secondly, there exists SNR penalty resulting with increase in the fading parameter, η , as expected. For example, an ASER of 10^{-4} occurs at $P/N_0 \approx 24$ dB when $\eta_{sd} = \eta_{sr} = 1$, $\mu_{sd} = \mu_{sr} = \mu_{rd} = 1$, and $\kappa_{rd} = 1$, and $P/N_0 \approx 25$ dB when $\eta_{sd} = \eta_{sr} = 5$, $\mu_{sd} = \mu_{sr} = \mu_{rd} = 1$.

C. Impact of Power Allocation

Table II tabulates the fraction of the total power allocated to s for 4×2 -RQAM as a function of Ω_{rd} , $\eta_{sd} = \eta_{sr}$, $\mu_{sd} = \mu_{sr}$, κ_{rd} and μ_{rd} at $P/N_0 = 40$ dB. The values of the optimal power for any value of channel parameters of mixed η - μ and κ - μ fading channels can be obtained by solving either (37) or (38) using the software MATHEMATICA. From Fig. 5, we can see that

TABLE II
OPTIMAL POWER ALLOCATION FACTOR FOR 4×2 -RQAM WITH $\beta = 1$, $\Omega_{sd} = \Omega_{sr} = 1$ AND $P/N_0 = 40$ dB.

Ω_{rd}	$\mu_{rd} = 1,$ $\kappa_{rd} = 1$			$\mu_{sd} = \mu_{sr} = 1,$ $\eta_{sd} = \eta_{sr} = 1$		
	$\mu_{sd} = \mu_{sr}$	$\eta_{sd} = \eta_{sr}$	ξ	μ_{rd}	κ_{rd}	ξ
1	0.5	0.01	0.7760	0.5	1	0.8000
		1	0.6544		4	0.8000
	1	0.01	0.6706	1	1	0.6682
		1	0.6668		4	0.6679
10	0.5	0.01	0.9070	0.5	1	0.8000
		1	0.8228		4	0.8000
	1	0.01	0.6972	1	1	0.6682
		1	0.6682		4	0.6782

when fading parameters and variances of link are highly unbalance, an optimal power allocation is useful for dual-hop DF relaying system.

V. CONCLUSION

Novel closed-form expressions are obtained for the ASER of general order RQAM and XQAM schemes with dual-hop DF relaying systems over mixed η - μ and κ - μ fading channels. The derived ASER expressions are used to analyze the performance of various QAM schemes with dual-hop DF relaying systems over mixed η - μ and κ - μ fading. We obtain the asymptotic ASER, which is useful to determine the system behavior at high SNRs in terms of the diversity order. Applying the asymptotic expression, optimal power allocation between the source node and the relay node under a total power constraint is analyzed. It is illustrated by numerical examples that the ASER performance vary according to the fading parameters of the communication links. All numerical results are validated through computer simulation results.

APPENDIX

SOLUTION TO THE INTEGRALS: $\mathcal{I}_1(x, \phi)$, $\mathcal{I}_2(x, \phi)$, $\mathcal{I}_1^\infty(x, \phi)$ AND $\mathcal{I}_2^\infty(x, \phi)$

In the following subsections, we will derive the closed-form expressions for $\mathcal{I}_1(x, \phi)$, $\mathcal{I}_2(x, \phi)$, $\mathcal{I}_1^\infty(x, \phi)$ and $\mathcal{I}_2^\infty(x, \phi)$ in terms of multivariate Lauricella's $(F_D^{(n)}(\cdot), \Phi_1^{(n)}(\cdot))$ hypergeometric

functions which are given as [45], [46]

$$F_D^{(n)}(a, b_1, b_2, \dots, b_n; c; x_1, x_2, \dots, x_n) = \frac{1}{B(a, c-a)} \int_0^1 \frac{u^{a-1}(1-u)^{c-a-1}}{\prod_{i=1}^n (1-u x_i)^{b_i}} du$$

$$= \sum_{m_1, m_2=0, \dots, m_n=0}^{\infty} \frac{(a)_{\sum_i m_i}}{(c)_{\sum_i m_i}} \prod_{i=1}^n \frac{(b_i)_{m_i} x_i^{m_i}}{m_i!}; |x_1| < 1, |x_2| < 1 \dots |x_n| < 1 \quad (39)$$

and

$$\Phi_1^{(n)}(a, b_1, b_2, \dots, b_{n-1}; c; x_1, x_2, \dots, x_n) = \frac{1}{B(a, c-a)} \int_0^1 \frac{u^{a-1}(1-u)^{c-a-1} \exp(u x_n)}{\prod_{i=1}^{n-1} (1-u x_i)^{b_i}} du$$

$$= \sum_{m_1, m_2=0, \dots, m_n=0}^{\infty} \frac{(a)_{\sum_i m_i} \prod_{i=1}^{n-1} (b_i)_{m_i}}{(c)_{\sum_i m_i}} \prod_{i=1}^n \frac{x_i^{m_i}}{m_i!}, \quad (40)$$

where $B(a, b) = \int_0^1 x^{a-1}(1-x)^{b-1} dx$ is Beta function, $m_i! = \Gamma(m_i+1)$ and $(a)_n = \Gamma(a+n)/\Gamma(a)$ is the Pochhammer symbol for $n \geq 0$. The $F_D^{(n)}(\cdot)$, and $\Phi_1^{(n)}(\cdot)$ functions can be easily and accurately evaluated by using its finite integral representation or its infinite series representation.

A. Closed-form Expression for $\mathcal{I}_1(x, \pi/2)$

Substituting (12) into (21) and followed by $u = \cos^2 \theta$, the closed-form expression for the integral $\mathcal{I}_1(x, \pi/2)$ can be given as [43]

$$\mathcal{I}_1(x, \pi/2) = \frac{\Gamma(2\mu_{sd} + 0.5) \mathcal{M}_{\gamma_{sd}}(x^2/2)}{2\sqrt{\pi} \Gamma(2\mu_{sd} + 1)} F_D^{(2)} \left(0.5, \mu_{sd}, \mu_{sd}; 2\mu_{sd} + 1; \frac{4\mu_{sd}(h_{sd} - H_{sd})}{4\mu_{sd}(h_{sd} - H_{sd}) + x^2 \bar{\gamma}_{sd}}, \right.$$

$$\left. \frac{4\mu_{sd}(h_{sd} + H_{sd})}{4\mu_{sd}(h_{sd} + H_{sd}) + x^2 \bar{\gamma}_{sd}} \right). \quad (41)$$

B. Closed-form Expression for $\mathcal{I}_1(x, \text{arccot}(y/x))$

Substituting (12) into (21) and followed by $u = 1 - (y^2/x^2) \tan^2 \theta$, the closed-form expression for the integral $\mathcal{I}_1(x, \text{arccot}(y/x))$ can be given as [43]

$$\mathcal{I}_1(x, \text{arccot}(y/x)) = \frac{x y \mathcal{M}_{\gamma_{sd}} \left(\frac{x^2 + y^2}{2} \right)}{2\pi(x^2 + y^2)(2\mu_{sd} + 0.5)} F_D^{(3)} \left(1, 1, \mu_{sd}, \mu_{sd}; 2\mu_{sd} + 1.5; \frac{x^2}{x^2 + y^2}, \right.$$

$$\left. \frac{4\mu_{sd}(h_{sd} - H_{sd}) + x^2 \bar{\gamma}_{sd}}{4\mu_{sd}(h_{sd} - H_{sd}) + (x^2 + y^2) \bar{\gamma}_{sd}}, \frac{4\mu_{sd}(h_{sd} + H_{sd}) + x^2 \bar{\gamma}_{sd}}{4\mu_{sd}(h_{sd} + H_{sd}) + (x^2 + y^2) \bar{\gamma}_{sd}} \right). \quad (42)$$

C. Closed-form Expression for $\mathcal{I}_2(x, \pi/2)$

Substituting, (12) and (13) into (22) followed by $t = \frac{2\mu_{rd}^2\kappa_{rd}(1+\kappa_{rd})\sin^2\theta}{2\mu_{rd}(1+\kappa_{rd})\sin^2\theta+x^2\bar{\gamma}_{rd}}$, and $u = \left(\frac{2\mu_{rd}(1+\kappa_{rd})+x^2\bar{\gamma}_{rd}}{2\mu_{rd}^2\kappa_{rd}(1+\kappa_{rd})}\right)t$, respectively, the closed-form expression for the integral $\mathcal{I}_2(x, \pi/2)$ can be given as

$$\begin{aligned} \mathcal{I}_2(x, \pi/2) &= \frac{\exp(-\mu_{rd}\kappa_{rd})\Gamma(2\mu_{sd} + \mu_{rd} + 0.5)x(2\mu_{rd}(1 + \kappa_{rd}))^{\mu_{rd}}(4\mu_{sd}\sqrt{h}(\bar{\gamma}_{rd}/\bar{\gamma}_{sd}))^{2\mu_{sd}}\sqrt{\bar{\gamma}_{rd}}}{2\sqrt{\pi}\Gamma(2\mu_{sd} + \mu_{rd} + 1)(x^2\bar{\gamma}_{rd} + 2\mu_{rd}(1 + \kappa_{rd}))^{2\mu_{sd} + \mu_{rd} + 0.5}} \\ &\times \Phi_1^{(4)}\left(2\mu_{sd} + \mu_{rd} + 0.5, 1, \mu_{sd}, \mu_{sd}; 2\mu_{sd} + \mu_{rd} + 1; \frac{2\mu_{rd}(1 + \kappa_{rd})}{x^2\bar{\gamma}_{rd} + 2\mu_{rd}(1 + \kappa_{rd})}, \right. \\ &\frac{2\mu_{rd}(1 + \kappa_{rd})\bar{\gamma}_{sd} - 4\mu_{sd}(h_{sd} - H_{sd})\bar{\gamma}_{rd}}{x^2\bar{\gamma}_{sd}\bar{\gamma}_{rd} + 2\mu_{rd}(1 + \kappa_{rd})\bar{\gamma}_{sd}}, \frac{2\mu_{rd}(1 + \kappa_{rd})\bar{\gamma}_{sd} - 4\mu_{sd}(h_{sd} + H_{sd})\bar{\gamma}_{rd}}{x^2\bar{\gamma}_{sd}\bar{\gamma}_{rd} + 2\mu_{rd}(1 + \kappa_{rd})\bar{\gamma}_{sd}}, \\ &\left. \frac{2\mu_{rd}^2\kappa_{rd}(1 + \kappa_{rd})}{x^2\bar{\gamma}_{rd} + 2\mu_{rd}(1 + \kappa_{rd})}\right). \end{aligned} \quad (43)$$

D. Closed-form Expression for $\mathcal{I}_2(x, \text{arccot}(y/x))$

Substituting, (12) and (13) into (22) followed by $t = \frac{2\mu_{rd}^2\kappa_{rd}(1+\kappa_{rd})\sin^2\theta}{2\mu_{rd}(1+\kappa_{rd})\sin^2\theta+x^2\bar{\gamma}_{rd}}$, and $u = \left(\frac{2\mu_{rd}(1+\kappa_{rd})+(x^2+y^2)\bar{\gamma}_{rd}}{2\mu_{rd}^2\kappa_{rd}(1+\kappa_{rd})}\right)t$, respectively, the closed-form expression for the integral $\mathcal{I}_2(x, \text{arccot}(y/x))$ can be given as

$$\begin{aligned} \mathcal{I}_2(x, \text{arccot}(y/x)) &= \frac{\exp(-\mu_{rd}\kappa_{rd})x\sqrt{\bar{\gamma}_{rd}}(2\mu_{sd} + \mu_{rd} + 0.5)^{-1}(2\mu_{rd}(1 + \kappa_{rd}))^{\mu_{rd}}}{2\pi(4\mu_{sd}\sqrt{h}(\bar{\gamma}_{rd}/\bar{\gamma}_{sd}))^{-2\mu_{sd}}((x^2 + y^2)\bar{\gamma}_{rd} + 2\mu_{rd}(1 + \kappa_{rd}))^{2\mu_{sd} + \mu_{rd} + 0.5}} \\ &\times \Phi_1^{(5)}\left(2\mu_{sd} + \mu_{rd} + 0.5, 1, 0.5, \mu_{sd}, \mu_{sd}; 2\mu_{sd} + \mu_{rd} + 1.5; \frac{2\mu_{rd}(1 + \kappa_{rd})}{(x^2 + y^2)\bar{\gamma}_{rd} + 2\mu_{rd}(1 + \kappa_{rd})}, \right. \\ &\frac{x^2\bar{\gamma}_{rd} + 2\mu_{rd}(1 + \kappa_{rd})}{(x^2 + y^2)\bar{\gamma}_{rd} + 2\mu_{rd}(1 + \kappa_{rd})}, \frac{2\mu_{rd}(1 + \kappa_{rd})\bar{\gamma}_{sd} - 4\mu_{sd}(h_{sd} - H_{sd})\bar{\gamma}_{rd}}{(x^2 + y^2)\bar{\gamma}_{sd}\bar{\gamma}_{rd} + 2\mu_{rd}(1 + \kappa_{rd})\bar{\gamma}_{sd}}, \\ &\left. \frac{2\mu_{rd}(1 + \kappa_{rd})\bar{\gamma}_{sd} - 4\mu_{sd}(h_{sd} + H_{sd})\bar{\gamma}_{rd}}{(x^2 + y^2)\bar{\gamma}_{sd}\bar{\gamma}_{rd} + 2\mu_{rd}(1 + \kappa_{rd})\bar{\gamma}_{sd}}, \frac{2\mu_{rd}^2\kappa_{rd}(1 + \kappa_{rd})}{(x^2 + y^2)\bar{\gamma}_{rd} + 2\mu_{rd}(1 + \kappa_{rd})}\right). \end{aligned} \quad (44)$$

E. Closed-form Expression for $\mathcal{I}_1(x, \arctan(y/z))$

Substituting (12) into (21) and followed by $u = 1 - (z^2/y^2)\tan^2\theta$, the closed-form expression for the integral $\mathcal{I}_1(x, \arctan(y/z))$ can be given as [43]

$$\begin{aligned} \mathcal{I}_1(x, \arctan(y/z)) &= \frac{yz\mathcal{M}_{\gamma_{sd}}\left(\frac{x^2(y^2+z^2)}{2y^2}\right)}{2\pi(y^2 + z^2)(2\mu_{sd} + 0.5)}F_D^{(3)}\left(1, 1, \mu_{sd}, \mu_{sd}; 2\mu_{sd} + 1.5; \frac{y^2}{y^2 + z^2}, \right. \\ &\left. \frac{4\mu_{sd}(h_{sd} - H_{sd})y^2 + x^2y^2\bar{\gamma}_{sd}}{4\mu_{sd}(h_{sd} - H_{sd})y^2 + x^2(y^2 + z^2)\bar{\gamma}_{sd}}, \frac{4\mu_{sd}(h_{sd} + H_{sd})y^2 + x^2y^2\bar{\gamma}_{sd}}{4\mu_{sd}(h_{sd} + H_{sd})y^2 + x^2(y^2 + z^2)\bar{\gamma}_{sd}}\right). \end{aligned} \quad (45)$$

F. Closed-form Expression for $\mathcal{I}_2(x, \arctan(y/z))$

Substituting, (12) and (13) into (22) followed by $t = \frac{2\mu_{rd}^2\kappa_{rd}(1+\kappa_{rd})\sin^2\theta}{2\mu_{rd}(1+\kappa_{rd})\sin^2\theta+x^2\bar{\gamma}_{rd}}$, and $u = \left(\frac{2\mu_{rd}(1+\kappa_{rd})y^2+x^2(y^2+z^2)\bar{\gamma}_{rd}}{2\mu_{rd}^2\kappa_{rd}(1+\kappa_{rd})y^2}\right)t$, respectively, the closed-form expression for the integral $\mathcal{I}_2(x, \arctan(y/z))$ can be given as

$$\begin{aligned} \mathcal{I}_2(x, \arctan(y/z)) &= \frac{\exp(-\mu_{rd}\kappa_{rd})xy\sqrt{\bar{\gamma}_{rd}}(2\mu_{sd} + \mu_{rd} + 0.5)^{-1}(2y^2\mu_{rd}(1 + \kappa_{rd}))^{\mu_{rd}}}{2\pi (4y^2\mu_{sd}\sqrt{h}(\bar{\gamma}_{rd}/\bar{\gamma}_{sd}))^{-2\mu_{sd}}(x^2(y^2 + z^2)\bar{\gamma}_{rd} + 2y^2\mu_{rd}(1 + \kappa_{rd}))^{2\mu_{sd} + \mu_{rd} + 0.5}} \\ &\times \Phi_1^{(5)}\left(2\mu_{sd} + \mu_{rd} + 0.5, 1, 0.5, \mu_{sd}, \mu_{sd}; 2\mu_{sd} + \mu_{rd} + 1.5; \frac{2\mu_{rd}(1 + \kappa_{rd})y^2}{x^2(y^2 + z^2)\bar{\gamma}_{rd} + 2\mu_{rd}(1 + \kappa_{rd})y^2}, \right. \\ &\frac{x^2y^2\bar{\gamma}_{rd} + 2\mu_{rd}(1 + \kappa_{rd})y^2}{x^2(y^2 + z^2)\bar{\gamma}_{rd} + 2\mu_{rd}(1 + \kappa_{rd})y^2}, \frac{2\mu_{rd}(1 + \kappa_{rd})y^2\bar{\gamma}_{sd} - 4\mu_{sd}(h_{sd} - H_{sd})y^2\bar{\gamma}_{rd}}{x^2(y^2 + z^2)\bar{\gamma}_{sd}\bar{\gamma}_{rd} + 2\mu_{rd}(1 + \kappa_{rd})y^2\bar{\gamma}_{sd}}, \\ &\left. \frac{2\mu_{rd}(1 + \kappa_{rd})y^2\bar{\gamma}_{sd} - 4\mu_{sd}(h_{sd} + H_{sd})y^2\bar{\gamma}_{rd}}{x^2(y^2 + z^2)\bar{\gamma}_{sd}\bar{\gamma}_{rd} + 2\mu_{rd}(1 + \kappa_{rd})y^2\bar{\gamma}_{sd}}, \frac{2\mu_{rd}^2\kappa_{rd}(1 + \kappa_{rd})y^2}{x^2(y^2 + z^2)\bar{\gamma}_{rd} + 2\mu_{rd}(1 + \kappa_{rd})y^2}\right). \end{aligned} \quad (46)$$

G. Closed-form Expression for $\mathcal{I}_1^\infty(x, \pi/2)$

Substituting (28) into (32) and followed by $u = \cos^2\theta$, the closed-form expression for the integral $\mathcal{I}_1^\infty(x, \pi/2)$ can be given as

$$\mathcal{I}_1^\infty(x, \pi/2, \bar{\gamma}_{sd}) = \frac{B(0.5, 2\mu_{sd} + 0.5)}{2\pi (4\mu_{sd}\sqrt{h_{sd}}/(x^2\bar{\gamma}_{sd}))^{-2\mu_{sd}}}. \quad (47)$$

H. Closed-form Expression for $\mathcal{I}_2^\infty(x, \pi/2)$

Substituting, (28) and (29) into (33) followed by $u = \cos^2\theta$, respectively, the closed-form expression for the integral $\mathcal{I}_2^\infty(x, \pi/2)$ can be given as

$$\mathcal{I}_2^\infty(x, \pi/2) = \frac{B(0.5, 2\mu_{sd} + \mu_{rd} + 0.5) \exp(-\mu_{rd}\kappa_{rd})}{2\pi (4\mu_{sd}\sqrt{h_{sd}}/(x^2\bar{\gamma}_{sd}))^{-2\mu_{sd}}} \left(\frac{\mu_{rd}(1 + \kappa_{rd})}{x^2\bar{\gamma}_{rd}}\right)^{\mu_{rd}}. \quad (48)$$

I. Closed-form Expression for $\mathcal{I}_1^\infty(x, \operatorname{arccot}(y/x))$

Substituting (28) into (32) and followed by $u = 1 - (y^2/x^2)\tan^2\theta$, the closed-form expression for the integral $\mathcal{I}_1^\infty(x, \operatorname{arccot}(y/x))$ can be given as

$$\begin{aligned} \mathcal{I}_1^\infty(x, \operatorname{arccot}(y/x)) &= \left(\frac{4\mu_{sd}\sqrt{h_{sd}}}{(x^2 + y^2)\bar{\gamma}_{sd}}\right)^{2\mu_{sd}} \frac{xy}{2\pi(x^2 + y^2)} \\ &\times B(1, 2\mu_{sd} + 0.5) F_D^{(1)}\left(1, 2\mu_{sd} + 1; 2\mu_{sd} + 1.5; \frac{x^2}{x^2 + y^2}\right). \end{aligned} \quad (49)$$

J. Closed-form Expression for $\mathcal{I}_2^\infty(x, \text{arccot}(y/x))$

Substituting, (28) and (29) into (33) followed by $u = 1 - (y^2/x^2) \tan^2 \theta$, the closed-form expression for the integral $\mathcal{I}_2^\infty(x, \text{arccot}(y/x))$ can be given as

$$\begin{aligned} \mathcal{I}_2^\infty(x, \text{arccot}(y/x)) &= \left(\frac{4\mu_{sd}\sqrt{h_{sd}}}{(x^2 + y^2)\bar{\gamma}_{sd}} \right)^{2\mu_{sd}} \frac{\exp(-\mu_{rd}\kappa_{rd})xy B(1, 2\mu_{sd} + \mu_{rd} + 0.5)}{2\pi(x^2 + y^2)((x^2 + y^2)\bar{\gamma}_{rd}/(\mu_{rd}(1 + \kappa_{rd})))^{\mu_{rd}}} \\ &\times F_D^{(1)} \left(1, 2\mu_{sd} + \mu_{rd} + 1; 2\mu_{sd} + \mu_{rd} + 1.5; \frac{x^2}{x^2 + y^2} \right). \end{aligned} \quad (50)$$

K. Closed-form Expression for $\mathcal{I}_1^\infty(x, \arctan(y/z))$

Substituting (28) into (32) and followed by $u = 1 - (y^2/z^2) \tan^2 \theta$, the closed-form expression for the integral $\mathcal{I}_1^\infty(x, \arctan(y/z))$ can be given as

$$\begin{aligned} \mathcal{I}_1^\infty(x, \arctan(y/z)) &= \left(\frac{4y^2\mu_{sd}\sqrt{h_{sd}}}{x^2(y^2 + z^2)\bar{\gamma}_{sd}} \right)^{2\mu_{sd}} \frac{zy}{2\pi(y^2 + z^2)} \\ &\times B(1, 2\mu_{sd} + 0.5) F_D^{(1)} \left(1, 2\mu_{sd} + 1; 2\mu_{sd} + 1.5; \frac{y^2}{y^2 + z^2} \right). \end{aligned} \quad (51)$$

L. Closed-form Expression for $\mathcal{I}_2^\infty(x, \arctan(y/z))$

Substituting, (28) and (29) into (33) followed by $u = 1 - (z^2/y^2) \tan^2 \theta$, the closed-form expression for the integral $\mathcal{I}_2^\infty(x, \arctan(y/z))$ can be given as

$$\begin{aligned} \mathcal{I}_2^\infty(x, \arctan(y/z)) &= \left(\frac{4y^2\mu_{sd}\sqrt{h_{sd}}}{x^2(y^2 + z^2)\bar{\gamma}_{sd}} \right)^{2\mu_{sd}} \frac{\exp(-\mu_{rd}\kappa_{rd})zyB(1, 2\mu_{sd} + \mu_{rd} + 0.5)}{2\pi(y^2 + z^2)(x^2(y^2 + z^2)\bar{\gamma}_{rd}/(y^2\mu_{rd}(1 + \kappa_{rd})))^{\mu_{rd}}} \\ &\times F_D^{(1)} \left(1, 2\mu_{sd} + \mu_{rd} + 1; 2\mu_{sd} + \mu_{rd} + 1.5; \frac{y^2}{y^2 + z^2} \right). \end{aligned} \quad (52)$$

REFERENCES

- [1] A. Sendonaris, E. Erkip, and B. Aazhang, "User cooperation diversityPart I: System description,"*IEEE Trans. Commun.*, vol. 51, no. 11, pp. 1927-1938, Nov. 2003.
- [2] J. N. Laneman, D. N. C. Tse, and G.W.Wornell, "Cooperative diversity in wireless networks: Efficient protocols and outage behaviour," *IEEE Trans. Inf. Theory*, vol. 50, no. 12, pp. 3062-3080, Dec. 2004.
- [3] M. Salem, A. Adinoyi, H. Yanikomeroglu, and D. Falconer, "Opportunities and challenges in OFDMA-based cellular relay networks: A radio resource management perspective,"*IEEE Trans. Veh. Technol.*, vol. 59, no. 5, pp. 2496-2510, Jun. 2010.
- [4] A. So and B. Liang, "Enhancing WLAN capacity by strategic placement of tetherless relay points,"*IEEE Trans. Mobile Comput.*, vol. 6, no. 5, pp. 522-535, May 2007.

- [5] M. Abouelseoud and A. Nosratinia, "Hybrid relay selection in heterogenous relay networks," in *Proc. IEEE ASILOMAR*, Pacific Grove, CA, USA, Nov. 2010, pp. 1864-1868.
- [6] T. Q. Duong, H. Shin, and E.-K. Hong, "Effect of line-of-sight on dualhop nonregenerative relay wireless communications," in *Proc. IEEE VTC*, Baltimore, MD, USA, May 2007, pp. 571-575.
- [7] H. A. Suraweera, R. H. Y. Louie, Y. Li, G. K. Karagiannidis, and B. Vucetic, "Two hop amplify-and-forward transmission in mixed Rayleigh and Rician fading channels," *IEEE Commun. Lett.*, vol. 13, no. 4, pp. 227-229, Apr. 2009.
- [8] H. A. Suraweera, G. K. Karagiannidis, and P. J. Smith, "Performance analysis of the dual-hop asymmetric fading channel," *IEEE Trans. Wireless Commun.*, vol. 8, no. 6, pp. 2783-2788, Jun. 2009.
- [9] P. Herath, U. Gunawardana, R. Liyanapathirana, and N. Rajatheva, "Mixed Rayleigh and Rician fading with partial relay selection," in *Proc. IEEE ICSPCS*, Gold Coast, Australia, Dec. 2010, pp. 1-4.
- [10] H. Ding, J. Ge, D. B. da Costa, and Y. Guo, "Outage analysis for multiuser two-way relaying in mixed Rayleigh and Rician fading," *IEEE Commun. Lett.*, vol. 15, no. 4, pp. 410-412, Apr. 2011.
- [11] A. K. Gurung, F. S. Al-Qahtani, Z. M. Hussain, and H. Alnuweiri, "Performance analysis of amplify-forward relay in mixed Nakagami-m and Rician fading channels," in *Proc. IEEE ATC*, Ho Chi Minh City, Vietnam, Oct. 2010, pp. 321-326.
- [12] W. Xu, J. Zhang, Y. Liu, and P. Zhang, "Performance analysis of semi-blind amplify-and-forward relay system in mixed Nakagami-m and Rician fading channels," *IEICE Trans. on Commun.*, vol. E93-B, no. 11, pp. 3137-3140, Nov. 2010.
- [13] K. P. Peppas, G. C. Alexandropoulos, and P. T. Mathiopoulos, "Performance analysis of dual-hop AF relaying systems over mixed η - μ and κ - μ fading channels," *IEEE Trans. Veh. Technol.*, vol. 62, no. 7, pp. 3149-3163, Sep. 2013.
- [14] S. S. Soliman, and N. C. Beaulieu, "The bottleneck effect of Rician fading in dissimilar dual-hop AF relaying systems," *IEEE Trans. Veh. Technol.*, vol. 63, no. 4, pp. 1957-1965, May 2014.
- [15] N. Kapucu, M. Bilim and Ibrahim Develi, "Outage probability analysis of dual-hop decode-and-forward relaying over mixed Rayleigh and generalized Gamma fading channels," *Wireless Pers. Commun.*, vol. 72, pp. 947-954, Sep. 2012.
- [16] C. Yang, W. Wang, S. Zhao, and Mugen Peng, "Opportunistic decode-and-forward cooperation in mixed Rayleigh and Rician fading channels," *ETRI Journal*, vol. 33, no. 2, pp. 287-290, Apr. 2011.
- [17] P. Kumar and K. Dhaka "Performance analysis of a decode-and-forward relay system in κ - μ and η - μ fading channels," early access article in *IEEE Trans. Veh. Technol.*
- [18] P. Kyosti, J. Meinila, L. Hentila, X. Zhao, T. Jamsa, C. Schneider, M. Narandzi, M. Milojevi, A. Hong, J. Ylitalo, V.-M. Holappa, M. Alatossava, R. Bultitude, Y. deJong, and T. Rautiainen, WINNER II interim channel models (IST-4-027756 WINNER II D1.1.1 V1.1), WINNER II, Munich, Germany, Tech. Rep. [Online]. Available: [http:// www.ist-winner.org/WINNER2-Deliverables/D1.1.1.pdf](http://www.ist-winner.org/WINNER2-Deliverables/D1.1.1.pdf)
- [19] W. Su, A. K. Sadek, and R. J. K. Liu, "SER performance analysis and optimum power allocation for decode-and-forward cooperation protocol in wireless networks," in *Proc. IEEE WCNC*, Mar. 2005, vol. 2, pp. 984-989.
- [20] A. K. Sadek, W. Su, and R. J. K. Liu, "Performance analysis for multinode decode-and-forward relaying in cooperative wireless networks," in *Proc. IEEE ICASSP*, Mar. 18-23, 2005, vol. 3, pp. iii/521-iii/524.
- [21] S. Ikki and M. H. Ahmed, "Performance of decode-and-forward cooperative diversity networks over Nakagami-m fading channels," in *Proc. IEEE GLOBECOM*, Nov. 2007, pp. 4328-4333.
- [22] Y. Lee and M.-H. Tsai, "Performance of decode-and-forward cooperative communications over Nakagami-m fading channels," *IEEE Trans. Veh. Technol.*, vol. 58, no. 3, pp. 1218-1228, Mar. 2009.
- [23] Y. G. Kim, and N. C. Beaulieu, "Exact closed-form solutions for the BEP of decode-and-forward cooperative systems in Nakagami-m fading channels," *IEEE Trans. Commun.*, vol. 59, no. 9, pp. 2355-2361, Sep. 2010.

- [24] Q. Shi and Y. Karasawa, "Error probability of opportunistic decode-and-forward relaying in Nakagami- m fading channels with arbitrary m ," *IEEE Wireless Commun. Lett.*, vol. 2, no. 1, pp. 86-89, Feb. 2013.
- [25] K. Yang, J. Yang, J. Wu, and C. Xing, and Y. Zhou, "Performance analysis of DF cooperative diversity system with OSTBC over spatially correlated Nakagami- m fading channels," *IEEE Trans. Veh. Technol.*, vol. 63, no. 3, pp. 1270-1281, Mar. 2014.
- [26] Y. Lu, and N. Yang, "Symbol error rate of decode-and-forward relaying in two-wave with diffuse power fading channels," *IEEE Trans. Wireless Commun.*, vol. 11, no. 10, pp. 3412-3417, Oct. 2012.
- [27] M. K. Fikadu, P. C. Sofotasios, M. Valkama and Q. Cui, "Analytic Performance Evaluation of M-QAM Based Decode-and-Forward Relay Networks over enriched multipath fading channels ", in *Proc. IEEE WiMob'14*, Larnaca, Cyprus, pp. 194-199, Oct. 2014.
- [28] A. Muller and J. Speidel, "Exact symbol error probability of M -PSK for multihop transmission with regenerative relays," *IEEE Commun. Lett.*, vol. 11, no. 12, pp. 952-954, Dec. 2007.
- [29] J. Cao, L.-L. Yang, and Z. Zhong, "Performance analysis of multihop wireless links over Generalized- K fading channels," *IEEE Trans. Veh. Technol.*, vol. 61, no. 4, pp. 1590-1598, May 2012.
- [30] D. Dixit, and P. R. Sahu, "Performance of multihop communication systems with regenerative relays in η - μ fading channels," in *Proc. IEEE 79th VTC*, Seoul, South Korea, May 2014, pp. 1-5.
- [31] N. C. Beaulieu, and J. Hu, "A closed-form expression for the outage probability of decode-and-forward relaying in dissimilar Rayleigh fading channels," *IEEE Commun. Lett.*, vol. 10, no. 12, pp. 813-815, Dec. 2006.
- [32] H. A. Suraweera, P. J. Smith, and J. Armstrong, "Outage probability of cooperative relay networks in Nakagami- m fading channels," *IEEE Commun. Lett.*, vol. 10, no. 12, pp. 834-836, Dec. 2006.
- [33] C. K. Datsikas, N. C. Sagias, F. I. Lazarakis, and G. S. Tombras, "Outage analysis of decode-and-forward relaying over Nakagami- m fading channels," *IEEE Signal Process. Lett.*, vol. 15, pp. 41-44, Jan. 2008.
- [34] W.-G. Li, H.-M. Chen, and M. Chen, "Outage probability of dual-hop decode-and-forward relaying systems over generalized fading channels," *Eur. Trans. Telecommun.*, vol. 21, no. 1, pp. 86-89, Jan. 2010.
- [35] W.-G. Li, "Outage capacity of dual-hop decode-and-forward relaying system over generalized fading channels," in *Proc. IEEE ICFCC*, Nanjing, China, May 2010, pp. V3-827-V3-831.
- [36] M. D. Yacoub, "The κ - μ distribution and the η - μ distribution," *IEEE Antennas. Propag. Mag.*, vol. 49, no. 1, pp. 68-81, Feb. 2007.
- [37] J. G. Proakis, *Digital Communications*, 4th ed. New York: McGraw-Hill, 2001.
- [38] J. G. Smith, "Odd-bit quadrature amplitude shift keying," *IEEE Trans. Commun.*, vol. 23, no. 3, pp. 385-389, Mar. 1975.
- [39] S. Abrar and I. Qureshi, "Blind equalization of cross-QAM signals," *IEEE Signal Process. Lett.*, vol. 13, no. 12, pp. 745-748, Dec. 2006.
- [40] S. Panigrahi and T. Le-Ngoct, "Fine-granularity loading schemes using adaptive Reed-Solomon coding for discrete multitone modulation systems," in *Proc. IEEE ICC'05*, vol. 2 Seoul, Korea, May 2005, pp. 1352-1356.
- [41] M. Zwingenstein-Colin, M. Gzalet and M. Gharbi, "Non-iterative bit-loading algorithm for ADSL-type DMT applications," *IEE Proc.-Commun.*, vol. 150, no. 6, pp. 414-418, 2003.
- [42] H. Yu, G. Wei, F. Ji and X. Zhang, "On the error probability of cross-QAM with MRC reception over generalized $\eta - \mu$ fading channels," *IEEE Trans. Veh. Technol.*, vol. 60, no. 6, pp. 2631-2643, Jul. 2011.
- [43] N. Y. Ermolova, "Useful integrals for performance evaluation of communication systems in generalized η - μ and κ - μ fading channels," *IET Commun.*, vol. 3, no. 2, pp. 303-308, Feb. 2009.

- [44] D. Dixit, and P. R. Sahu, "Performance of QAM signaling over TWDP fading channels," *IEEE Trans. Wireless Commun.*, vol. 12, no. 4, pp. 1794-1799, Apr. 2013.
- [45] H. Exton, *Multiple hypergeometric functions and applications*, New York: Wiley, 1976.
- [46] F. J. Lopez-Martinez, R. F. Pawula, E. Martos-Naya, and J. F. Paris, "A clarification of the proper-integral form for the Gaussian Q -function and some new results involving the F-function," *IEEE Commun. Lett.*, vol. 18, no. 9, pp. 1495-1498, Sep. 2014.
- [47] D. Morales-Jimenez and J. F. Paris, "Outage probability analysis for η - μ fading channels," *IEEE Commun. Lett.*, vol. 14, no. 6, pp. 521-523, Jun. 2010.
- [48] A. P. Prudnikov, Y. A. Brychkov, O. I. Marichev, *Integrals and series* Gordon and Breach Science Publishers, 1986, vol. 4.
- [49] M. K. Simon and M.-S. Alouini, *Digital Communication over Fading Channels*, 2nd ed. New York: Wiley, 2005.
- [50] N. C. Beaulieu, "A useful integral for wireless communication theory and its application to rectangular signaling constellation error rates," *IEEE Trans. Commun.*, vol. 54, no. 5, pp. 802-805, May 2006.
- [51] Y. Song, H. Shin, and E.-K. Hong, "MIMO cooperative diversity with scalar-gain amplify-and-forward relaying" *IEEE Trans. Commun.*, vol. 57, no. 7, pp. 1932-1938, Jul. 2009.